

1  
2  
3  
4  
5  
6  
7  
8  
9  
10  
11  
12  
13  
14  
15  
16

Supplementary Information for

**Non-mercury catalytic acetylene hydrochlorination over  
bimetallic Au-Ba(II)/AC catalysts**

Haiyang Zhang,<sup>a</sup> Wei Li,<sup>a</sup> Xueqin Li,<sup>a</sup> Wei Zhao,<sup>a</sup> Junjie Gu,<sup>a</sup> Xueyan Qi,<sup>a</sup>  
Yanzhao Dong,<sup>a</sup> Bin Dai,<sup>b</sup> and Jinli Zhang<sup>\*a,b</sup>

<sup>a</sup> School of Chemical Engineering & Technology, Tianjin University, Tianjin 300072,  
P.R. China.

<sup>b</sup> Key Laboratory for Green Processing of Chemical Engineering of Xinjiang Bingtuan,  
School of Chemistry and Chemical Engineering, Shihezi University, Xinjiang, Shihezi  
832000, P.R. China.

\* To whom correspondence may be addressed.

Tel.: +86-22-2789-0643; Fax: +86-22-2740-3389.

*E-mail address:* zhangjinli@tju.edu.cn (J.L. Zhang).

18 **Table of contents:**

19 **Catalyst characterization**

20 **Table S1.** The loss ratio of Au in Au-Ba(II)/AC catalysts, determined by ICP-AES.

21 **Table S2.** Weight loss of fresh and used Au/AC catalysts under different temperature  
22 ranges.

23 **Table S3.** Weight loss of fresh and used Au1Ba(II)1/AC catalysts under different  
24 temperature ranges.

25 **Table S4.** Size of Au particles in Au-Ba(II)/AC catalysts, determined by XRD <sup>a</sup>.

26 **Fig. S1.** (a) The schematic diagram of three different bimetallic catalysts prepared with  
27 different impregnation order of two precursors. (b) Catalytic performance of three kinds  
28 of bimetallic catalysts. Reaction conditions: T = 200 °C, GHSV(C<sub>2</sub>H<sub>2</sub>) = 360 h<sup>-1</sup>,  
29 V<sub>HCl</sub>/V<sub>C<sub>2</sub>H<sub>2</sub></sub> = 1.15.

30 **Fig. S2.** Catalytic performance of Au1Ba(II)1/AC in 86 h on stream. Reaction  
31 conditions: T = 200 °C, GHSV(C<sub>2</sub>H<sub>2</sub>) = 360 h<sup>-1</sup>, V<sub>HCl</sub>/V<sub>C<sub>2</sub>H<sub>2</sub></sub> = 1.15.

32 **Fig. S3.** Selectivity to VCM over the fresh Au-Ba(II)/AC catalysts.

33 **Fig. S4.** (a) C<sub>2</sub>H<sub>2</sub>- and (b) HCl- TPD profiles of the fresh Au-Ba(II)/AC catalysts.

34 **Fig. S5.** Isothermal adsorption-desorption curves of (a) fresh and (b) used catalysts.

35 **Fig. S6.** TG curves of the fresh and used Au-Ba(II)/AC catalysts.

36 **Fig. S7.** TEM images of (a, b) Au/AC and (c, d) Au1Ba(II)1/AC before (a, c) and after  
37 (b, d) reaction.

38 **Fig. S8.** Deconvolution profiles of Au 4f<sub>7/2</sub> XPS spectra for Au-Ba(II)/AC catalysts.

39 The spectra are relatively noisy because of low total loading of metals in the catalysts.

40 **References**

## 42 **Catalyst characterization**

43 Samples for examination by transmission electron microscopy (TEM) were prepared by  
44 dispersing the catalyst powder in high-purity ethanol, and then allowing a drop of the  
45 suspension to evaporate on a holey carbon film supported by a 300-mesh copper TEM  
46 grid. Bright-field and annular dark-field (ADF) imaging experiments were respectively  
47 carried out using a JEM2100F TEM instrument and an FEI Titan 80-300 TEM/STEM  
48 system equipped with a CEOS spherical aberration corrector.

49 X-ray photoelectron spectroscopy (XPS) was performed with a PHI5000 Versa Probe  
50 spectrometer using a monochromatised Al K $\alpha$  X-ray source (24.2 W) with an analyzer  
51 pass energy of 187.85 eV for survey scans and 46.95 eV for detailed elemental scans.  
52 Binding energies were referenced to the C1s binding energy of carbon, taken to be  
53 284.6 eV. As it is well known that cationic Au species can be reduced to the zero-valent  
54 state by secondary electron emission during XPS analysis, the Au(4f) region was  
55 recorded at the beginning and end of the analysis.<sup>1</sup> The Au<sup>3+</sup>, Au<sup>0-s</sup>, and Au<sup>0</sup> amounts  
56 are reported as the percentage of the total Au amount.

57 Au contents in the catalysts were determined using an inductively coupled plasma  
58 (ICP 725), using a Vista Chip IICCD detector, and the testing wavenumber is 242.794  
59 nm.

60 **Table S1** The loss ratio of Au in Au-Ba(II)/AC catalysts, determined by ICP-AES.

Catalyst	Au loading, wt %		Loss ratio of Au, %
	Fresh	Used	
Au/AC	0.908	0.899	0.99
Au1Ba(II)0.5/AC	0.915	0.906	0.98
Au1Ba(II)1/AC	0.918	0.910	0.87
Au1Ba(II)3/AC	0.912	0.902	1.10
Au1Ba(II)5/AC	0.907	0.898	0.99

62 **Table S2** Weight loss of fresh and used Au/AC catalysts under different temperature ranges.

Temperature (°C)	< 150	150-450	450-500	150-500
Weight loss of fresh sample, (%)	0.9	1.6	2.6	4.2
Weight loss of used sample, (%)	0.8	5.5	3.4	8.9

64 **Table S3** Weight loss of fresh and used Au1Ba(II)1/AC catalysts under different temperature ranges.

Temperature (°C)	< 150	150-400	400-450	150-450
Weight loss of fresh sample, (%)	1.0	3.6	2.7	6.3
Weight loss of used sample, (%)	0.6	6.4	2.8	9.2

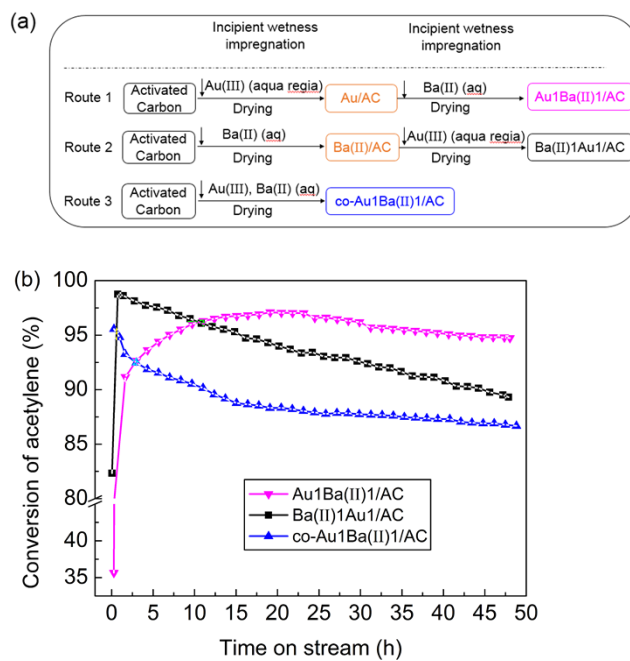
**Table S4** Size of Au particles in Au-Ba(II)/AC catalysts, determined by XRD <sup>a</sup>.

Catalyst	Au particles Size (nm)	
	Fresh	Used
Au/AC	23	36±3
Au1Ba(II)0.5/AC	32	33±3
Au1Ba(II)1/AC	<4 <sup>b</sup>	21±3
Au1Ba(II)3/AC	<4 <sup>b</sup>	32±3
Au1Ba(II)5/AC	<4 <sup>b</sup>	23±3

<sup>a</sup> Error estimated from XRD peak broadening of 0.06° at the Au (111) reflection at 38.10° ( $2\theta$ ).

<sup>b</sup> It was impossible to assign any error band below 4 nm, as this size is below the XRD method.





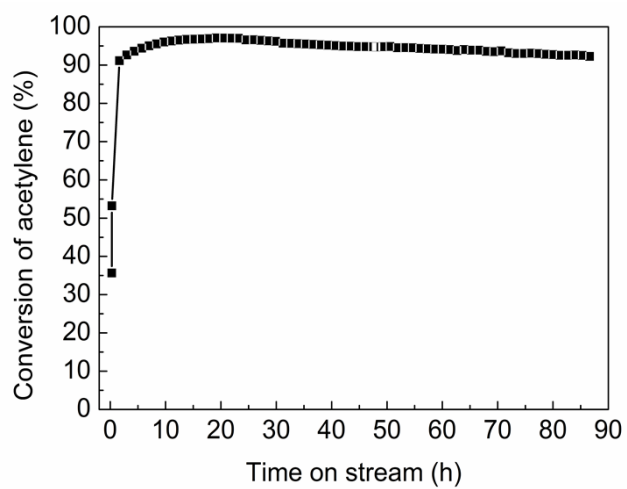
68

69 **Fig. S1.** (a) The schematic diagram of three different bimetallic catalysts prepared with different

70 impregnation order of two precursors. (b) Catalytic performance of three kinds of bimetallic

71 catalysts. Reaction conditions:  $T = 200\text{ }^{\circ}\text{C}$ ,  $\text{GHSV}(\text{C}_2\text{H}_2) = 360\text{ h}^{-1}$ ,  $V_{\text{HCl}}/V_{\text{C}_2\text{H}_2} = 1.15$ .

72

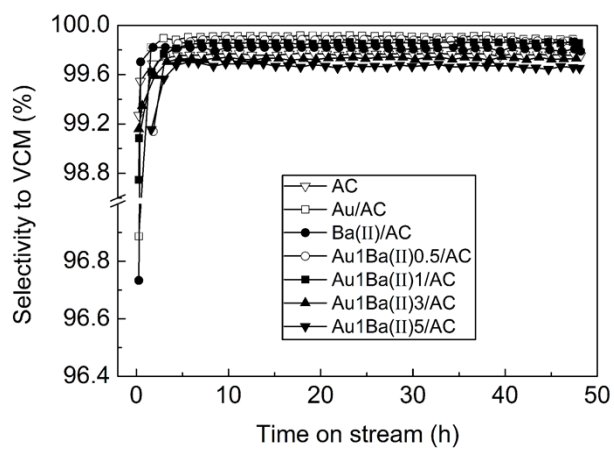


73

74 **Fig. S2.** Catalytic performance of Au1Ba(II)1/AC in 86 h on stream. Reaction conditions: T = 200

75

°C, GHSV(C<sub>2</sub>H<sub>2</sub>) = 360 h<sup>-1</sup>, V<sub>HCl</sub>/V<sub>C<sub>2</sub>H<sub>2</sub></sub> = 1.15.



76

77

**Fig. S3.** Selectivity to VCM over the fresh Au-Ba(II)/AC catalysts.

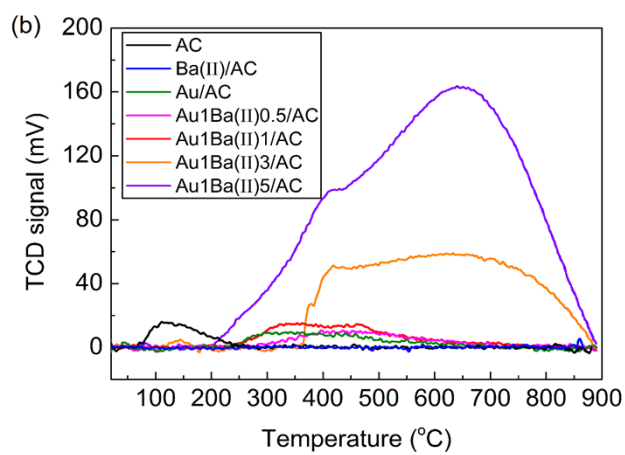
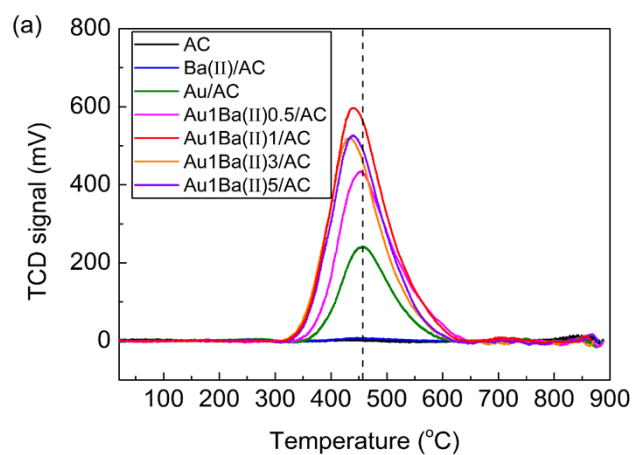
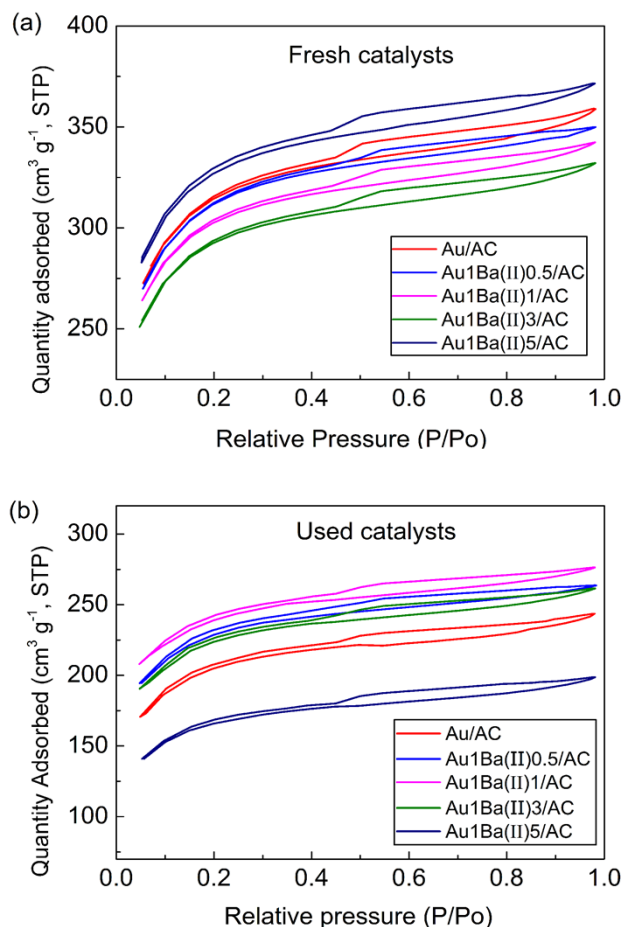


**Fig. S4.** (a)  $C_2H_2$ - and (b)  $HCl$ - TPD profiles of the fresh Au-Ba(II)/AC catalysts.

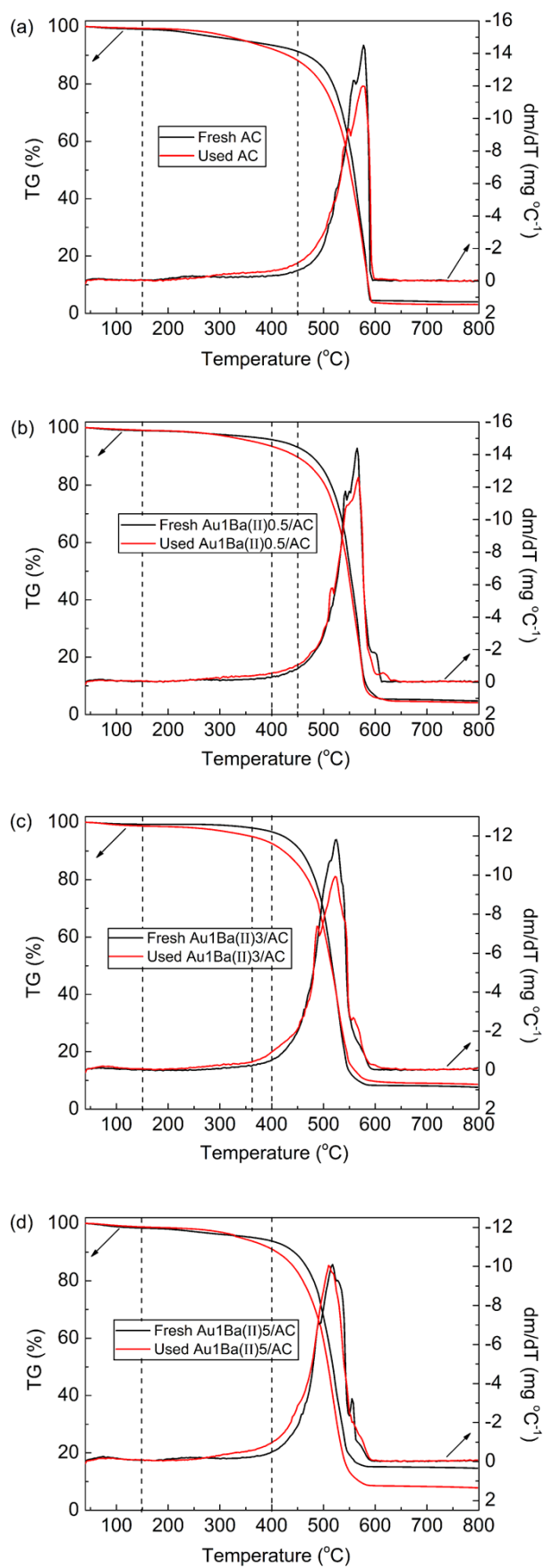


81

82 **Fig. S5.** Isothermal adsorption-desorption curves of (a) fresh and (b) used catalysts.

83 It can be seen from Fig. S5 that all of the samples exhibit type I isotherms with an H4  
 84 adsorption-desorption hysteresis loop based on IUPAC nomenclature, which is typically  
 85 attributed to adsorption in the micropore.

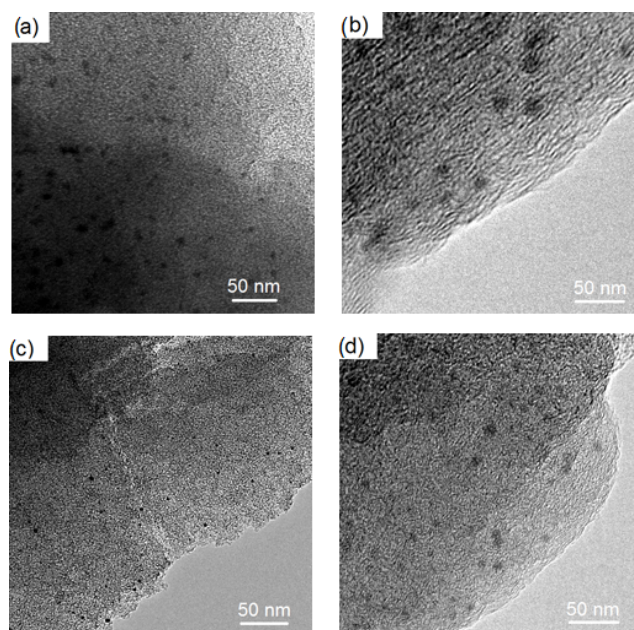
86 The limiting adsorption quantity may sometimes indicate the monolayer adsorption  
 87 capacity; it may also be the quantity that fills the pore volume for microporous  
 88 adsorbents. The adsorption volume of each catalyst decreases after the  
 89 hydrochlorination reaction (Fig. S5b), which is due to pore blockage brought about by  
 90 carbon deposition or collapse. The adsorption of Au1Ba(II)1/AC changes minimally  
 91 before and after the reaction, which indicates that the amount of carbon deposition or  
 92 the degree of collapse in Au1Ba(II)1/AC is lower than that in other used catalysts.



93

94

**Fig. S6.** TG curves of the fresh and used Au-Ba(II)/AC catalysts.

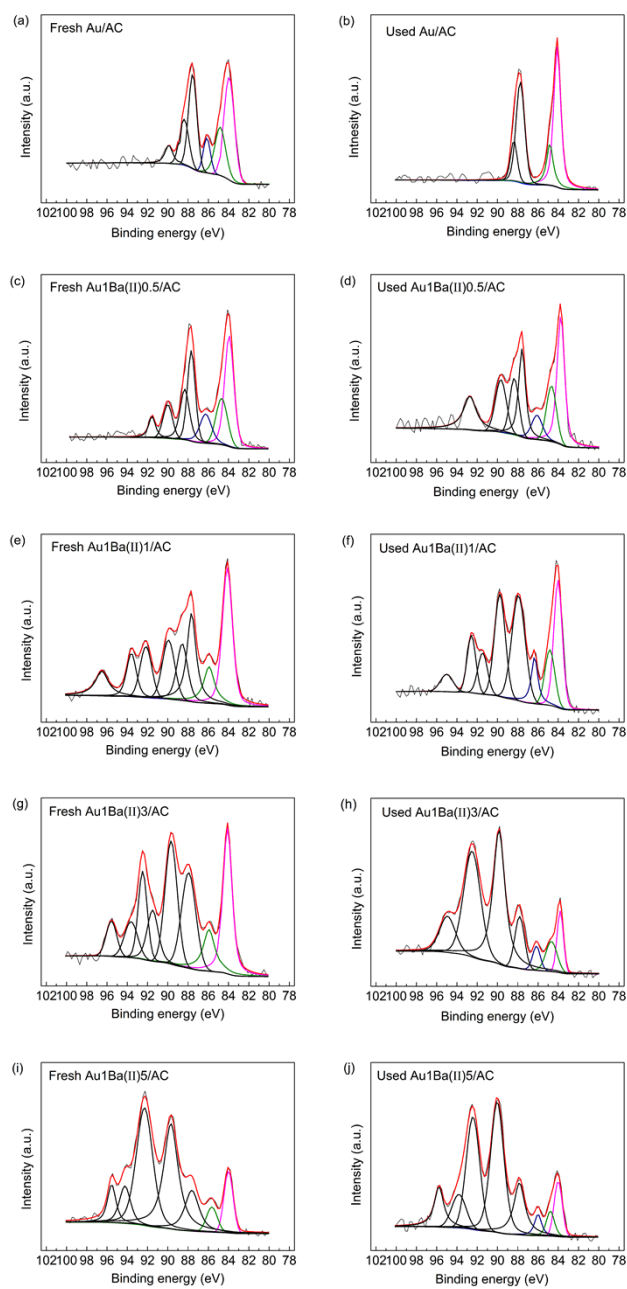


95

96 **Fig. S7.** TEM images of (a, b) Au/AC and (c, d) Au<sub>1</sub>Ba(II)<sub>1</sub>/AC before (a, c) and after (b, d)

97

reaction.



98

99 **Fig. S8.** Deconvolution profiles of XPS Au 4f<sub>7/2</sub> spectra for Au-Ba(II)/AC catalysts. The spectra are

100

relatively noisy because of low total loading of metals in the catalysts.

## 101 **References**

- 102 1. Y. Fong, B. R. Visser, J. R. Gascooke, B. C. C. Cowie, L. Thomsen, G. F. Metha, M. A.  
 103 Buntine and H. H. Harris, *Langmuir*, 2011, **27**, 8099-8104.

104